The method of cycle-slip detection and repair GNSS meaturements by using receiver with high stability frequency oscillator

Nikolai S. KOSAREV*, Konstantin M. ANTONOVICH,
Leonid A. LIPATNIKOV

Siberian State University of Geosystems and Technologies,
10 Plakhotnogo St., Novosibirsk, 630108 Russia;
e-mail: kosarevnsk@yandex.ru, kaf.astronomy@ssga.ru, lipatnikov_l@mail.ru

Abstract: A method of phase GNSS measurement control is described. The method is based on comparison of geometric range increments which are calculated using measurement data and approximate receiver coordinates and satellite navigation message position taking into account troposphere and ionosphere correction increments. Applicability of moving average for phase GNSS measurement control to detect the cycle slips and outliers is demonstrated. Test results of cycle slip detecting in phase measurements made by the receiver with high stability frequency oscillator are provided.

Key words: GNSS, receiver, measurement, carrier phase, cycle slip, moving average, geometric range

1. Introduction

The main objective of GNSS measurement quality check is to detect cycle slips in carrier phase, to correct them. Also outliers, which may be caused by multipath, and other various types of interference, can be eliminated by replacing measured value with smoothed value.

Carrier phase cycle slips occur when the receiver of the GNSS user loses the signal. Cycle slips may be evident, when the observation pause continues for several epochs, or non-evident when the observation restarts before the next observation epoch occurs. In any case there occurs an error for entire cycles value in phase observation ΔN, but still the fractional part remains

---

*corresponding author: tel. 8-913-706-9195, e-mail: kosarevnsk@yandex.ru

the same as if there was no cycle slip (*Rizos, 1997; Seeber, 2003; Xu, 2003; Hofmann-Wellenhof et al., 2008; Joosten and Tiberius, 2000; Antonovich, 2005*).

There are two ways for solving problem of GNSS measurement quality control. The first one is measurement hardware and technique improvement for minimizing the number of cycle slips. The second one is development of mathematical methods for outliers detection and correction of cycle slips (*Kosarev, 2012*).

The improvement of satellite GNSS receivers' hardware includes ongoing receiving antennas design refinement and digital signal processing methods development. The improvement of mathematical GNSS quality control methods involves selection of approximating functions, code and phase pseudorange combination analysis etc. (*Kosarev, 2012*).

The works *Bastos and Landau (1988)*, *Cross and Ahmad (1988)*, *Collin and Warnant (1995)*, *Gao and Li, 1999)*, *Colombo et al. (1999)*, *Bisnath (2000)*, *Bisnath et al. (2001)*, *Banville and Langley (2010)*, *Banville and Langley (2012)* demonstrate cycle slips and outliers detection methods based on dual difference frequency difference analysis. The evident drawback of these methods is that it is impossible to use them for single GNSS receivers. The use of inertial-aided navigation systems (INS) enables to detect carrier phase cycle slips (losses) in kinematic measurements (*Lee et al., 2003; Du and Gao, 2012*). The works *Melbourne (1985)*, *Wübbena (1985)*, *Blewitt (1989)*, *Blewitt (1990)*, *Goad and Yang (1994)* describe outliers detection methods based on code and phase pseudoranges differences, phase pseudorange and iono-free combination differences, and time measurement differences.

The works *Zhalilo (2003, 2007)*, *Zhalilo and Sadanova (2004)* demonstrate the detailed research of Ukrainian scientists devoted to outliers detection methods that were proposed earlier.

There are a number of publications by A. S. Tolstikov and D. V. Stubarev (*Stubarev and Tolstikov, 2004; Stubarev, 2006a,b; Stubarev, 2008a,b*) which devoted to methods of outliers detection based on imitation modelling using measurement data imitator ModBis24, which is developed in Siberian Scientific Research Institute of Metrology.

The algorithm for outlier detection is based on analyzing difference between phase measurements and reference trajectory. Smoothing by Cheby-

shev polynomials, Kalman filtering and robust processing procedures are applied.

For detection and editing cycle slips and outliers authors of the present article developed a technique for GNSS measurements quality control based on computation of geometric range increment using approximate coordinates of the station and orbit of the satellite. The distinction of the proposed technique from the aforementioned ones is that here we use differences between two successive measurements epochs and compare them to their modeled values which can be obtained with higher precision than phase measurements if some conditions are satisfied. Those conditions refer to measurement interval, accuracy of station's position and satellite orbit. The most important condition is that the GNSS receiver is equipped with highly stable atomic frequency standard (*Antonovich and Kosarev, 2011; Antonovich and Kosarev, 2012a,b*).

2. Theory

The code pseudoranges P_i (meters) and carrier phase ϕ_i (cycles) for frequency bands $L1$, $L2$ at moments (measurement epochs) t_i, $i = 1, \ldots, n$ separated by interval Δt. Phase differences $\Delta \phi$ between two successive epochs are determined as follows (*Antonovich and Kosarev, 2011; Antonovich and Kosarev, 2012a,b*):

$$\Delta \phi_{i,i+1}(L1) = \phi_{i+1} - \phi_i = \frac{1}{\lambda_{L1}} \Big[\Delta \rho_{i,i+1} - \Delta I_{i,i+1} + \Delta T_{i,i+1} +$$
$$+ \Delta \delta m_{i,i+1} + (A1(r)_{i,i+1} - A1(s)_{i,i+1}) \cdot \Delta t \Big], \quad (1)$$

where: $\Delta \rho$ – geometric range shift;

ΔI – ionospheric delay shift;

ΔT – tropospheric delay shift;

$\Delta \delta m$ – multipath influence shift on the phase measurement;

$A1(r), A1(s)$ – receiver and satellite clock rate;

λ – wavelength.

Topocentric distance increment (geometric range shift) $\Delta \rho$ is introduced as follows:

$$\Delta \rho_{i,i+1} = \rho_{i+1} - \rho_i \,, \tag{2}$$

where ρ_i calculated as:

$$\rho_i = \sqrt{(X - X_i)^2 + (Y - Y_i)^2 + (Z - Z_i)^2}\,. \tag{3}$$

In equation (3): station position is given in the earth-centered earth-fixed reference system, for example, by ITRS vector $\mathbf{R} = (X, Y, Z)^T$. Satellite position vectors $\mathbf{r_i} = (X_i, Y_i, Z_i)^T$ are calculated at the moments of signal emission t_i in the system time scale. According to definition of pseudorange P_i:

$$P_i = c\,(t_i' - t_i''), \tag{4}$$

where t_i' is the nominal moment in time scale implemented by the user's receiver clock, t_i'' – moments of signal transmission in the timescale of the GNSS satellite, c – speed of light in vacuum. Therefore, the moments t_i can be calculated according to formula:

$$t_i = t_i' - P_i/c + \mathrm{d}t_i^s. \tag{5}$$

Here $\mathrm{d}t_i^s$ is shift of space vehicle (SV) timescale relative to the system timescale at the moment of signal generation.

Algorithm for calculation of vectors $\mathbf{r_i}$ is provided in the Interface Control Document (*ICD-GPS-200C, 1993*). It is important to correct vectors $\mathbf{r_i}$ to take into account influence of rotation of the earth-centered earth-fixed (ECEF) reference frame during signal propagation from satellite to receiver i.e. Sagnac effect (*Rizos, 1997; Seeber, 2003; Xu, 2003*).

In papers *Antonovich and Kosarev (2012a,b)*, *Antonovich and Kosarev (2011)* authors consider using approximate station and satellite positions for calculation of geometric ranges increments. For demonstration of applicability of geometric ranges increments for phase measurements quality control let us introduce a geocentric reference system $O\xi\eta\zeta$ shown in Fig. 1. For the sake of simplicity fundamental plane $O\xi\eta$ coincides with orbital plane of the satellite which is in zenith of the station. In Fig. 1:

– O – center of Earth's mass (geocenter);
– ξ axis is aimed along radius vector R to the station A at which observations are made;
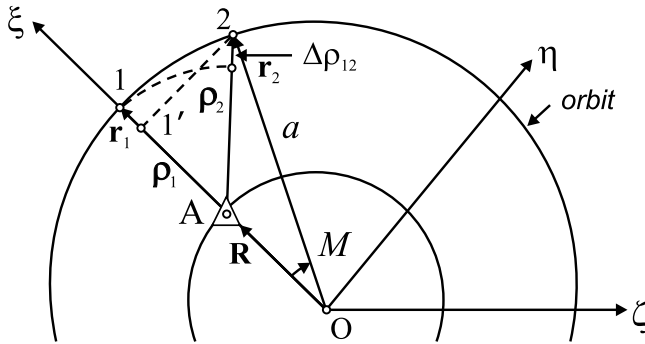– η axis lies in the orbital plane perpendicular to the radius vector of the station;

Fig. 1. Differerence of topocentric distances.

– ζ axis is perpendicular to the orbital plane.

Satellite orbit is considered circular, radius equals a. If disturbances are neglected, position $\mathbf{R}$ of the station and position of the satellite $\mathbf{r}_1$ at the moment t_1 can be presented as follows:

$$\mathbf{R} = \begin{bmatrix} R \\ 0 \\ 0 \end{bmatrix}, \quad \mathbf{r}_1 = \begin{bmatrix} a \\ 0 \\ 0 \end{bmatrix}. \tag{6}$$

Position of the satellite at t_2 can be calculated using following expressions:

$$\mathbf{r}_2 = \begin{bmatrix} a \cdot \cos M \\ a \cdot \sin M \\ 0 \end{bmatrix}, \tag{7}$$

$$M = n \cdot \Delta t, \tag{8}$$

where n is mean motion, $\Delta t = t_2 - t_1$, M – central angle (analogue of mean anomaly).

Then the topocentric vectors $\boldsymbol{\rho}_1$, $\boldsymbol{\rho}_2$ pointing to satellite at the moments t_1, t_2 are calculated according the formulae:

$$\boldsymbol{\rho}_1 = \mathbf{r}_1 - \mathbf{R} = \begin{bmatrix} a - R \\ 0 \\ 0 \end{bmatrix}, \quad \boldsymbol{\rho}_2 = \mathbf{r}_2 - \mathbf{R} = \begin{bmatrix} a \cdot \cos M - R \\ a \cdot \sin M \\ 0 \end{bmatrix}. \tag{9}$$

Scalars of vectors i.e. geometric ranges:

$$\rho_1 = |a - R|, \quad \rho_2 = \left| [a^2 - 2aR\cos M + R^2]^{1/2} \right|. \tag{10}$$

Topocentric range difference between the two epochs:

$$\Delta\rho = \rho_2 - \rho_1 = [a^2 - 2aR\cos M + R^2]^{1/2} - (a - R). \tag{11}$$

Assume small errors $d\xi$, $d\eta$, and $d\zeta$, such that real position of the station is defined by the formula:

$$\mathbf{R}' = \begin{bmatrix} R + d\xi \\ d\eta \\ d\zeta \end{bmatrix}. \tag{12}$$

New topocentric vectors:

$$\boldsymbol{\rho}'_1 = \mathbf{r}_1 - \mathbf{R}' = \begin{bmatrix} a - R - d\xi \\ -d\eta \\ -d\zeta \end{bmatrix}, \tag{13}$$

$$\boldsymbol{\rho}'_2 = \mathbf{r}_2 - \mathbf{R}' = \begin{bmatrix} a \cdot \cos M - R - d\xi \\ a \cdot \sin M - d\eta \\ -d\zeta \end{bmatrix}, \tag{14}$$

and correspondingly their scalars are:

$$\rho'_1 = |\mathbf{r}_1 - \mathbf{R}'| = \left[(a - R - dd\xi)^2 + d\eta^2 + d\zeta^2 \right]^{1/2}, \tag{15}$$

$$\rho'_2 = |\mathbf{r}_2 - \mathbf{R}'| = \left\{ [a\cos M - R - d\xi]^2 + (a\sin M - d\eta)^2 + d\zeta^2 \right\}^{1/2}. \tag{16}$$

Applying first-order Taylor expansion for (15) and (16) by $d\xi$, $d\eta$, $d\zeta$, one may get:

$$\rho'_1 = \rho_1 - d\xi, \tag{17}$$

$$\rho'_2 = \rho_2 - d\xi(a\cos M - R)/\rho_2 - d\eta\, a\sin M/\rho_2. \tag{18}$$

Formula (18) shows no influence of $d\zeta$ error in the first-order approximation. Then the difference of new topocentric distances can be expressed in the following way:

$$\Delta\rho' = \rho_2' - \rho_1' = \rho_2 - \rho_1 - \mathrm{d}\xi(a\cos M - R)/\rho_2 + \mathrm{d}\xi - \mathrm{d}\eta\, a\sin M/\rho_2 \,, \quad (19)$$

Deviation of this difference from the true value caused by errors in relative position of the stations and in orbit of the satellite equals to:

$$\nabla\Delta\rho = \Delta\rho' - \Delta\rho = -\mathrm{d}\xi(a\cos M - R)/\rho_2 + \mathrm{d}\xi - \mathrm{d}\eta a\sin M/\rho_2 \,. \quad (20)$$

Expanding trigonometric functions of angle M to series, using (20), yields:

$$\nabla\Delta\rho = \Delta\rho' - \Delta\rho = -\mathrm{d}\xi\Big(a\big[1 - (n\Delta t)^2/2\big] - R\Big)\big/\rho_2 + \mathrm{d}\xi - \mathrm{d}\eta\, a(n\Delta t)/\rho_2. \quad (21)$$

The Table 1 contains values of topocentric range changes depending on errors $\mathrm{d}\xi$, $\mathrm{d}\eta$, and also on interval Δt. Calculation was carried assuming $a = 26560\,\mathrm{km}$, $R = 6378\,\mathrm{km}$, $n = 30°/\mathrm{hr}$.

Table 1. The dependence of the geometric range increments errors on mutual satellite and station positions errors and time interval.

Errors of satellite – station relative position (M)	Geometric range increments error (mm) in time interval Δt (sec)							
	$\Delta t = 1$	$\Delta t = 2$	$\Delta t = 5$	$\Delta t = 10$	$\Delta t = 20$	$\Delta t = 30$	$\Delta t = 60$	$\Delta t = 600$
$\mathrm{d}\xi = \mathrm{d}\eta = 1$	0.2	0.5	1	2	4	6	11	107
$\mathrm{d}\xi = \mathrm{d}\eta = 5$	1	2	5	10	19	29	57	540
$\mathrm{d}\xi = \mathrm{d}\eta = 10$	1.9	3.8	9.5	19	38	57	114	1079

It is evident from Table 1 that in many cases influence of coordinate errors is below the noise level of P-code measurements (nearly 0.3 m).

The change of tropospheric delay between the two epochs can be represented by the formula:

$$\Delta T_{i,i+1} = T_z(\operatorname{cosec}\varepsilon_{i+1} - \operatorname{cosec}\varepsilon_i)\,, \quad (22)$$

with standard deviation:

$$\sigma_{\Delta T} = \sigma_{T_z}(\operatorname{cosec}\varepsilon_{i+1} - \operatorname{cosec}\varepsilon_i)\,, \quad (23)$$

with σ_{T_z} of about 0.2–0.4 m (*Antonovich, 2005*).

Changes of ionospheric delay can be calculated using formulae:

$$\Delta I_{L1,i,i+1} = \bar{I}_{L1,v}(F_{i+1} - F_i), \quad \Delta I_{L2,i,i+1} = \bar{I}_{L2,v}(F_{i+1} - F_i)\,. \quad (24)$$

where F – obliquity factor, $\bar{I}_{L1,v}$ and $\bar{I}_{L2,v}$ averaged vertical ionospheric delays $I_{L1,v,i}$, $I_{L2,v,i}$ at some interval between the epochs t_{i_1} and t_{i_2}:

$$\bar{I}_{L1,v} = \frac{1}{i_2 - i_1} \sum_{i_1}^{i_2} I_{L1,v,i}, \quad \bar{I}_{L2,v} = \frac{1}{i_2 - i_1} \sum_{i_1}^{i_2} I_{L2,v,i}. \tag{25}$$

Vertical ionospheric delays $I_{L1,v,i}$, $I_{L2,v,i}$ at epochs t_i for frequency bands $L1$ and $L2$ calculated as:

$$I_{L1,v,i} = \frac{I_{L1,i}}{F_i} = k \cdot \frac{P_{L2,i} - P_{L1,i}}{F_i}, \quad I_{L2,v,i} = \frac{f_{L1}^2}{f_{L2}^2} I_{L1,v,i}. \tag{26}$$

To minimize vertical ionospheric delays errors one can perform additional averaging through different satellites data. It's especially important in case if there are no P-code measurements.

The formulae for root mean square (RMS) deviations $\sigma_{\Delta I, L1}$, $\sigma_{\Delta I, L2}$ for differential ionospheric delays can be represented by the formula:

$$\begin{aligned}
\sigma_{\Delta I, L1, i, i+1} &= \frac{k(F_{i+1} - F_i)}{F_i \sqrt{i_2 - i_1}} \sqrt{2} \sigma_P, \\
\sigma_{\Delta I, L2, i, i+1} &= \frac{f_{L1}^2}{f_{L2}^2} \frac{k(F_{i+1} - F_i)}{F_i \sqrt{i_2 - i_1}} \sqrt{2} \sigma_P.
\end{aligned} \tag{27}$$

The formulae show that ionosphere model errors depend mostly on root mean square error of code pseudorange σ_P, which in its turn depends on equipment-specific noise level and on the type of code measurements (*Leick, 1995*).

Multipath modelling is a complicated issue. It has quasiperiodic nature. Amplitude can reach 5–6 cm and its period is 5 minutes or larger (*Leick, 1995*).

Table 2 contains modelled values of changes in tropospheric and ionospheric delays, multipath effect and their RMS errors $\sigma_{\Delta T}$, $\sigma_{\Delta I}$, $\sigma_{\Delta \delta m}$ calculated given $\varepsilon \approx 15°$, $i_2 - i_1 = 1$.

Additional contribution to variance $\sigma_{\Delta \phi}^2$ is introduced by frequency instability of the satellite clock σ_f^s / f and of the station clock $\sigma_{f,r} / f$. They are random values. Their influence in equation (1) can be evaluated using the following formula:

$$\sigma_{\Delta t} = c \, \Delta t \, \frac{\sqrt{\sigma_{f,r}^2 + (\sigma_f^s)^2}}{f}. \tag{28}$$

Table 2. Influence of tropospheric and ionospheric refraction and multipath on phase pseudorange increments (mm).

Time interval	Tropospheric delay		Ionospheric delay			Multipath	
	ΔT	$\sigma_{\Delta T}$	ΔI	$\sigma_{\Delta I}$ (GPS P-code)	$\sigma_{\Delta I}$ (GLONASS C/A code)	$\Delta \delta m$	$\sigma_{\Delta \delta m}$
$\Delta t = $ 1 sec	1.3	0.4	5.2	0.1	1.6	1	1
$\Delta t = $ 10 sec	13	4.2	52	1.2	24.5	7	7
$\Delta t = $ 30 sec	40	12.4	160	3.6	72	21	21

For GLONASS satellites σ_f^s/f has order of $(1–5)\cdot 10^{-13}$ (*Xu, 2003*), which adds 1–5mm to $\sigma_{\Delta t}$ if $\Delta t = 30$ sec. Using receivers with highly stable atomic clocks is necessary to reduce the influence of receiver's clock error to a level comparable to satellite clock errors. Such atomic clocks are installed on some stations of International GNSS Service (IGS) and also on the stations of GNSS ground control segment. It is expected that small-scale atomic clocks with relative frequency instability of $5\cdot 10^{-12}$ on one hour interval may appear in field geodetic GNSS receivers soon (*Quantum SA 45s; Shkel, 2011*).

After accounting for all mentioned effects formula (1) may be rewritten as follows:

$$\Delta\phi_{i,i+1}(L1) = \frac{1}{\lambda_{L1}}[(\rho_{i+1}-\rho_i)-\bar{I}_{L1}(F_{i+1}-F_i)+T_z(\text{cosec } \varepsilon_{i+1}-\text{cosec } \varepsilon_i)].\quad(29)$$

Expression for $L2$ band will have analogous form. Noise of phase measurements in those equations is neglected because it does not exceed 3 mm.

Increments $\Delta\phi_i$ modelled according to formula (29) generally are not equal to increments $\Delta\widetilde{\phi}_i$ calculated using measurements. Let us calculate discrepancies v_i (frequency band designation is omitted):

$$v_i = \Delta\phi_i - \Delta\widetilde{\phi}_i. \quad (30)$$

We fill further consider v_i consisting of systematic and random parts:

$$v_i = \Delta d_i + \Delta\varepsilon_i, \quad (31)$$

$$\Delta d_i = E(v_i), \quad (32)$$

291

where Δd_i is increment of systematic error of GNSS phase measurements model equal to mathematical expectation $E(v_i)$; $\Delta \varepsilon_i$ is an estimate of random change of error on the interval with zero mathematical expectation.

Systematic part of the error Δd_i can be found by smoothing discrepancies v_i in the window $[i-k, \, i+k]$:

$$\Delta d_i = \bar{v}_{[i-k,i+k]} \, . \tag{33}$$

Smoothing of discrepancies is proposed to be performed using moving average. The smoothed value will lag by k intervals. Median filtering is applied to avoid influence of outliers on the estimate of mathematical expectation (*Stubarev and Tolstikov, 2004; Stubarev, 2006a,b; Stubarev, 2008a,b; Stubarev, 2010*). Unpredictable effects including both cycle slips and other outliers in GNSS measurements, can emerge in random error part $\Delta \varepsilon_i$:

$$\Delta \varepsilon_i = v_i - \Delta d_i \, . \tag{34}$$

RMS σ_i is calculated using Bessel's formula:

$$\sigma_i = \sqrt{\frac{\sum\limits_{j=i-k}^{i+k} \Delta \varepsilon_j^2}{2k}} \, . \tag{35}$$

Value $\Delta \varepsilon_i$ is considered an outlier if the following conditions are satisfied:

$$|\Delta \varepsilon_i| > 2 \cdot \sigma_i \, , \quad |\Delta \varepsilon_i| > \Sigma \, , \tag{36}$$

where Σ is RMS error of measurement increment modelling by formula:

$$\Sigma = \sqrt{\sigma_{\Delta T}^2 + \sigma_{\Delta I}^2 + \sigma_{\Delta \rho}^2 + \sigma_{\Delta t}^2} \, . \tag{37}$$

If an outlier is identified, it can be corrected. If $\Delta \varepsilon_i$ magnitude is larger than the wavelength, it means that a cycle slip has occurred. It is well-known that in case of cycle slip all further phase measurements are biased by integer number of cycles but its fractional part is unaffected. Therefore, one can calculate corrected measurement $\bar{\phi}_i$ using formula:

$$\bar{\phi}_i = \text{int}(\phi_i) + \text{frac}(\widetilde{\phi}_i) \, , \tag{38}$$

where 'int' is an operator for separation of integer part of the value, a 'frac' – extraction of fractional part.

If the cycle slip has occurred previously, restoring can be performed according to formula:

$$\bar{\phi}_{i+1} = \widetilde{\phi}_i + \Delta\phi_{i+1} + \Delta d_{i+1}\,, \tag{39}$$

where $\bar{\phi}_{i+1}$ – smoothed value; $\widetilde{\phi}_i$ – measured value at previous epoch. Systematic part of the error Δd_{i+1} can be extrapolated linearly.

3. Experiment 1

Let us analyze the discrepancies through the GNSS measurement results, obtained at Mendeleevo station on January 1st, 2013. The measurements results files are available on the website of the International GNSS Service (IGS) datacenters. The station is equipped with dual-frequency and double system GNSS-receiver Topcon NetR3, connected to hydrogen frequency standard. The interval of measurements is 30 s. The station coordinates was get from RINEX file, the GPS satellite coordinates errors were estimated by difference between precise and navigational ephemerids of 1.5 m, and GLONASS satellites – about 3 m. Two GPS and two GLONASS satellites were chosen for the experiment. Observation session was nearly one hour. Satellite tracks were in different parts of observer's celestial sphere (see Table 3).

Table 3. Trajectories of the satellites.

GNSS	Satellite	UT time		Elevation of satellite	
		t_{start}	t_{end}	$\varepsilon_{\text{start}}$	ε_{end}
GPS	G1	22^h52^m	23^h46^m	$17°$	$7°$
GPS	G13	15^h00^m	16^h00^m	$52°$	$82°$
GLONASS	R1	7^h00^m	8^h00^m	$15°$	$48°$
GLONASS	R19	$0^h00.5^m$	$0^h55.5^m$	$68°$	$40°$

The calculations were performed using MATLAB 6.5 software. To calculate discrepancies we used the moving average with averaging window covering 7 epochs. Fig. 2 shows results for GPS G1 satellite ($L1$ frequency), Fig. 3 – for GLONASS R9 satellite ($L1$ frequency).
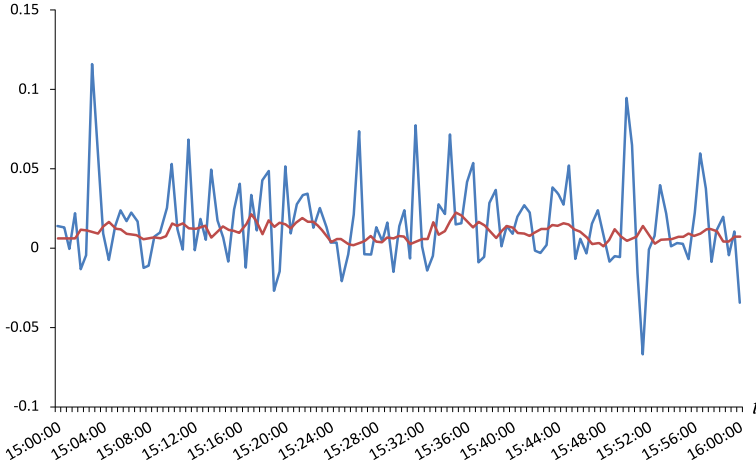
Fig. 2. Result of GPS G13 phase data filtration. Phase discrepancy in meters: blue – measured minus predicted, red – smoothed discrepancy.
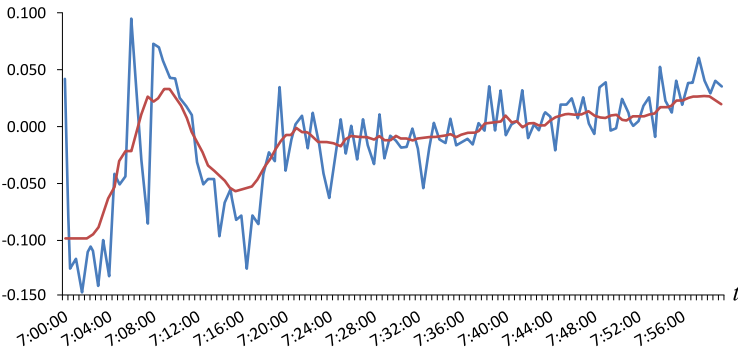

Fig. 3. Result of GLONASS R19 phase data filtration. Phase discrepancy in meters: blue – measured minus predicted, red – smoothed discrepancy.

Then the filtering procedure for cycle slips detection and correction was tested on evident and non-evident cycle slips, which were modeled. To model the evident cycle slip for the satellite G13 a 5-minute data gap was created. Then the slip ΔN was introduced into phase data:

$$\Delta N = \text{int}(P_{\text{end}} - P_{\text{start}})/\lambda \,, \tag{40}$$

where P_{start} and P_{end} are the P-code pseudorange values at the start and at

294

the end of data gap accordingly (Fig. 4a). To model the non-evident cycle loss the satellite GLONASS R1 data was used. The modeling was performed in the same way, but were chosen the neighboring values (Fig. 4b).

Then the data were restored by formula (39). To take into account the ionospheric delay the code pseudorange values were restored as well. The differences between the restored and initial carrier phase data are shown in Fig. 5.
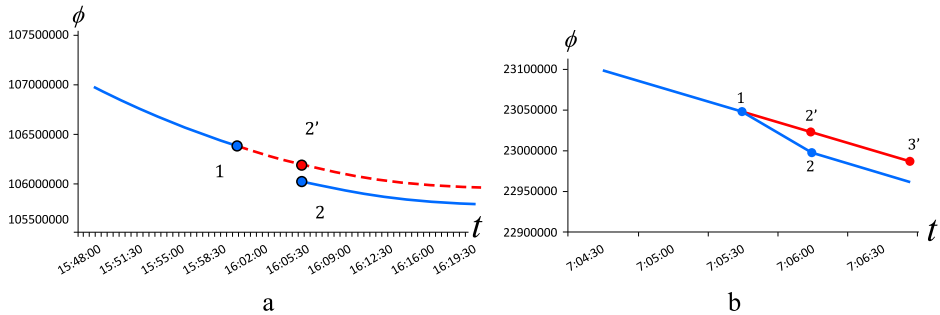

Fig. 4. The modeling of evident and non-evident carrier phase cycle loss: (a) for satellite GPS G13, (b) for satellite GLONASS R1. Where: 1 is the starting gap measurement point, 2 is the restarting measurement point. The blue color shows initial data, the red one is the restored data.
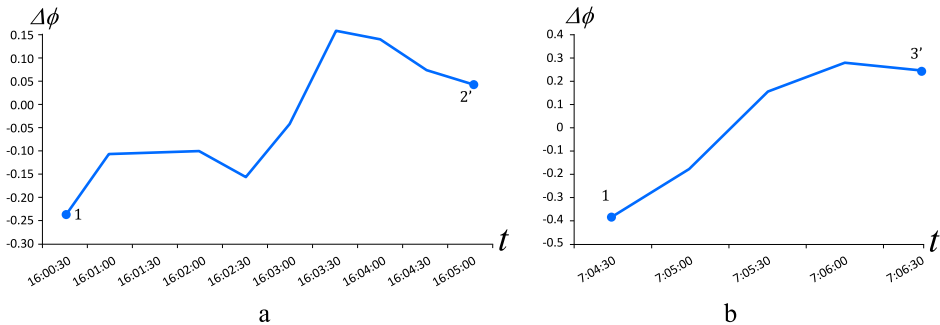

Fig. 5. The Differences between the really measured and modeled carrier phase (in cycles): (a) for satellite GPS G13, (b) for satellite GLONASS R1.

The analysis of Figs. 2–5 obviously shows that the application of median filtering for cycle counting losses detection enables to restore qualitative and reliable measurement data, provided by both GPS and GLONASS satellites. The application of the filter, based on median filtering, enables to definitely

and exactly detect cycle counting losses on the level of 5 cm, which is $^1/_4$ wave length.

4. Experiment 2

Validation of cycle slip and outlier detection based on moving average was conducted. For that purpose a numerical simulation was carried out. Non-evident cycle slips were randomly introduced into RINEX observation data.

Observation session was 6 hours. Measurements were performed using JAVAD Sigma G3T equipment with 1 sec interval. The receiver was connected to highly stable frequency standard Ch1-1006.

The data file obtained during the experiment was preprocessed using OCTAVA_PPA software, developed by Kharkov research group. Available version software allows you to process only GPS measurements. The aim was to eliminate non-modeled cycle slips and multipath effect in the test data (*Zhalilo and Sadanova, 2004*). Thus, etalon observation data were obtained which were not subject to those sources of errors.

Result of precision assessment of $L1$ and $L2$ phase measurements pre-processed using OCTAVA_PPA software is shown in figures 6 and 7 for all observed GPS satellite. Algorithms for preprocessing GPS measurements implemented in the OCTAVA_PPA software are given in the articles (*Zhalilo, 2003, 2007; Zhalilo and Sadanova, 2004*).

Figs. 6 and 7 show absence of cycle slips. It is seen the noise level is mostly within ± 2 cm.

Initial measurements interval was 1 sec. Thinned out datasets with 5 sec, 10 sec, 15 sec, 30 sec intervals were obtained by resampling down the initial dataset. Non-evident cycle slips were introduced into initial dataset and to the thinned out datasets using two approaches. The first approach consisted in introduction of cycle slips with magnitude of 1 cycle at random epochs. The second approach implied introduction of cycle slips (again magnitude was 1 cycle) into selected interval of observations in initial and resampled down datasets. Then the cycle slips were detected using the proposed technique. In Table 4 results of cycle slips detection are provided.

Results in Table 4 show that the technique enables reliable single cycle slips detection. It is important that the per cent of detected cycle slips is large independently on the interval of measurements if it does not exceed
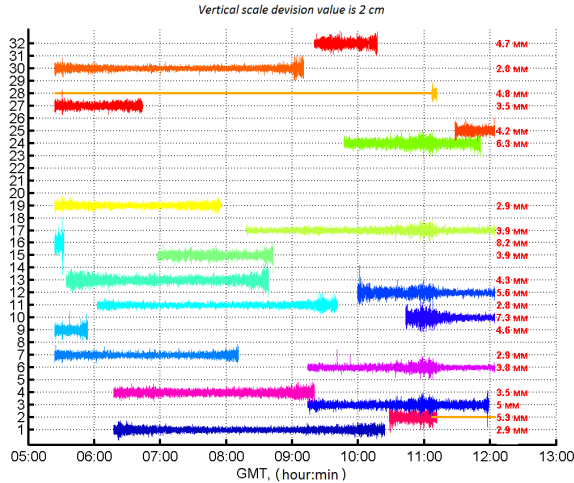
Fig. 6. Precision assessment of preprocessed $L1$ phase measurements for all observed GPS satellites.
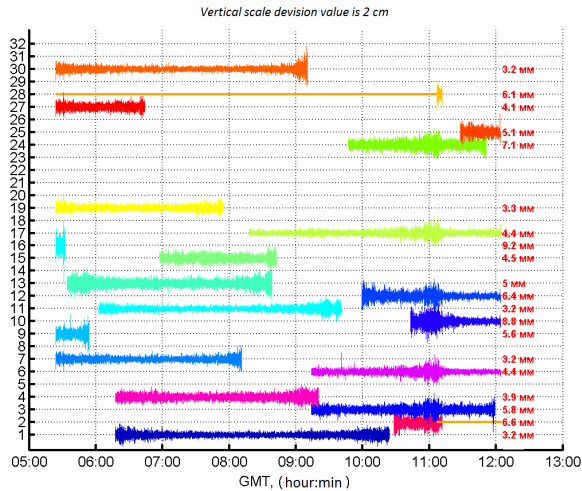

Fig. 7. Precision assessment of preprocessed $L2$ phase measurements for all observed GPS satellites.

30 s.

As it is evidently shown by Table 5 the technique allowed to detect nearly 100 % of single (one cycle) slips on the measurements interval up to 10 min.

297

Table 4. Results of detection of 1-cycle slips introduced into the etalon and resampled down datasets.

Measurements interval	Number of modeled single cycle slips		Portion of detected cycle slips	
	Totally	By satellite		
1 sec	700	G07 − 200	100 %	100 %
		G01 − 500		100 %
5 sec	400	G24 − 200	99 %	99 %
		G28 − 200		99 %
10 sec	200	G24 − 100	99 %	98 %
		G28 − 100		99 %
15 sec	200	G07 − 50	98 %	100 %
		G15 − 50		95 %
		G28 − 100		98 %
30 sec	100	G07 − 30	100 %	100 %
		G15 − 30		100 %
		G30 − 40		100 %

Table 5. Results of detection of single cycle slips introduced into the specific interval of the etalon datasets.

Measurements interval	Number of modelled single cycle slips introduced into selected time span	Portion of detected cycle slips
1 sec	G07 − 30 (30 sec)	100 %
1 sec	G07 − 60 (60 sec)	100 %
1 sec	G07 − 300 (5 min)	100 %
1 sec	G07 − 600 (10 min)	99 %

5. Conclusion

Application of GNSS receivers equipped with highly stable frequency generators opens new prospects for phase measurements quality control. The developed technique allows detection and correction of cycle slips and outliers. Unlike other techniques of phase measurements quality control based on search in observation space the proposed technique relies on calculation of geometric range and atmospheric effects increments. Those increments may be calculated using approximate coordinates of the station and the satellite

(the obtained using navigation message data). Increments of tropospheric and ionospheric delays are calculated using simple mapping functions. As a result of phase measurements quality control a file containing corrected values free of cycle slips and outliers can be obtained. Additionally an estimate of noise level for the dataset is provided which is necessary for quality assessment of measurements. This information can further be used for shaping measurements covariance matrix and improvement of solution accuracy in geodesy and navigation.

References

Antonovich K. I., 2005: The application of satellite radio-navigation systems in geodesy. Moscow, Kartgeocenter, Novosibirsk, Science, 334 p. (in Russian).

Antonovich K. I., Kosarev N. S., 2011: About one possibility of nonstop carrier phase control in GNSS observations. Interexpo GEO-Siberia – 2011, 19–29 April 2011, Novosibirsk, **1**, 2, SSGA, 2011, 164–168.

Antonovich K. I., Kosarev N. S., 2012a: Geometric range application for GNSS measurement control. Interexpo GEO-Siberia – 2012, **1**, 2, Geodesy, cartography, mine surveying: information package of scientific congress Interexpo GEO-Siberia – 2012, 10–20 April 2012, Novosibirsk, SSGA, 2012, 245–250.

Antonovich K. I., Kosarev N. S., 2012b: Method of code and phase pseudorange control in coordinate. High School publisher Geodesy and aerial photo survey, 2/1, 11–15 (in Russian).

Banville S., Langley R. B., 2010: Instantaneous cycle-slip correction for real-time PPP application. NAVIGATION, Journal of the Institute of Navigation, **57**, 4, 325–334.

Banville S., Langley R. B., 2012: Cycle slips correction for single-frequency PPP. In: Proceedings of the 25th International Technical Meeting of the Satellite Division of The Institute of Navigation (ION GNSS 2012), Nashville, TN, September 17–21, 2012, 3753–3761.

Bastos L., Landau H., 1988: Fixing cycle slips in dual-frequency kinematic GPS-applications using Kalman filtering. Manuscr. Geod., **13**, 4, 249–256.

Bisnath S. B., 2000: Efficient, automated cycle-slip correction of dual frequency kinematic GPS data. In: Proceedings of ION GPS 2000, Salt Lake City, Utah, 145–154.

Bisnath S. B., Kim D., Langley R. B., 2001: A new approach to an old problem: Carrier-phase cycle slips. GPS World, **12**, 5, 46–51.

Blewitt G., 1989: Carrier phase ambiguity resolution for the Global Positioning System applied to geodetic baselines up to 2000 km. J. Geophys. Res., **94**, B8, 10187–10203, `doi: 10.1029/JB094iB08p10187`.

Blewitt G., 1990: An automatic editing algorithm for GPS data. J. Geophys. Res., **17**, 3, 199–202, `doi: 10.1029/gl017i003p00199`.

Collin F., Warnant R., 1995: Application of wavelet transform for GPS cycle slip correction and comparison with Kalman filter. Manuscr. Geod., **20**, 3, 161–172.

Colombo O. L., Bhapkar U. V., Evans A. G., 1999: Inertial-aided cycle-slip detection/correction for precise, long-baseline kinematic GPS. In: Proceedings of the ION GPS, Nashville, TN, USA, September 14–17, 1999, 1915–1921.

Cross P. A., Ahmad N., 1988: Field validation of GPS phase measurements. GPS-Techniques Applied to Geodesy and Surveying, Groten E., Strauß R. (Eds.): Proceedings of the International GPS-Workshop, Darmstadt, April 10–13, 1988, 349–360.

Du S., Gao Y., 2012: Inertial aided cycle slip detection and identification for integrated PPP GPS and INS. Sensors 2012, **12**, 11, 14344–14362, available online: `https://www.ncbi.nlm.nih.gov/pmc/articles/PMC3522917/pdf/sensors-12-143 44.pdf`, `doi: 10.3390/s121114344`.

Gao Y., Li Z., 1999: Cycle slip detection and ambiguity resolution algorithms for dual-frequency GPS data processing. Mar. Geod., **22**, 3, 169–181, `doi: 10.1080/0149041 99273443`.

Goad C., Yang M., 1994: On automatic precision airborne GPS positioning. Proceedings of the International Symposium on Kinematic Systems in Geodesy, Geomatics and Navigation KIS'94, Banff, Alberta, Canada, August 30–September 2, 1994, 131–138.

Hofmann-Wellenhof B., Lichtenegger H., Wasle E., 2008: GNSS – Global Navigation Satellite Systems: GPS, GLONASS, Galileo and more. Wien, New-York: Springer, 516 p.

Interface Control Document ICD-GPS-200C, 1993: Navstar GPS Space Segment/Navigation User Interfaces. October 10, 1993–January 14, 2003, available online: `https:// navcen.uscg.gov/pubs/gps/icd200/ICD200Cw1234.pdf`.

Joosten P., Tiberius C. C. J. M., 2000: Fixing the ambiguities. Are you sure they're right? GPS World, **11**, 5, 46-51.

Kosarev N. S., 2012: Restoration of carrier phase: problems and decision ways. Vestnik of the Siberian State University of Geosystems and Technologies (SSUGT), **1**, 17, 53–59 (in Russian).

Lee H.-K., Wang J., Rizos C., 2003: Effective cycle slip detection and identification for high precision GPS/INS integrated systems. J. Navig., **56**, 3, 475–486, `doi: 10.1017 /S0373463303002443`.

Leick A., 1995: GPS Satellite Surveying. New York, Wiley-Interscience; 2nd ed., 560 p.

Melbourne W. G., 1985: The case for ranging in GPS based geodetic systems. In: Proceedings of the 1st International Symposium on Precise Positioning with the Global Positioning System, Goad C. (Ed.), Rockville, MD, USA, April 15–19, 1985, 373–386.

Quantum SA 45s Chip scale atomic clock. Available online: `https://www.microsemi.com/ document-portal/doc_download/133305-sa-45s-csac-datasheet`.

Rizos C., 1997: Principles and Practice of GPS Surveying. Monograph, School of Geomatic Engineering, The University of New South Wales, Sydney, available online: `http://www.sage.unsw.edu.au/sites/sage/files/SAGE_collection/MonographS eries/mono17.pdf`.

Seeber G., 2003: Satellite Geodesy. Berlin, New York: Walter de Gruyter, 589 p.

Shkel A. M., 2011: Microtechnology Comes of Age. GPS World, **22**, 9, 43–50.

Stubarev D. V., Tolstikov A. S., 2004: Algorithm for preliminary processing of pseudo-range measurements. In: Modern Problems of Radio Electronics. An Anthology, Krasnoyarsk State Technological University, Krasnoyarsk, 425–427 (in Russian).

Stubarev D. V., 2006a: Exclusion of outliers in results of trajectory observations. Stubarev D. V., Tolstikov A. S., Vestnik SGGA, **11**, Novosibirsk, SSGA, 25–29.

Stubarev D. V., 2006b: Smooth replenishment of missing trajectory observation data. Vestnik SGGA, **11**, Novosibirsk, SSGA, 33–38.

Stubarev D. V., 2008a: Study on algorithms for preliminary data processing using imitation modelling methods. Electronic resource: `http://www.jurnal.org/articles/2008/izmer11.html`.

Stubarev D. V., 2008b: Tasks of data preprocessing for requestless measurements (Zadachi predvaritel'noy obrabotki dannykh bezzaprosnykh izmereniy) Stubarev D. V., Tolstikov A. S., Proceedings of the IV International Congress Geo-Siberia 2008. Specialized instrument making, metrology, thermal physics, micromechanics. **4**, part 2., April 22–24 2008, Novosibirsk, SSGA, 150–153.

Stubarev D. V., 2010: Using imitation modelling methods for analysis of algorithms for preliminary processing of trajectory observation data. Stubarev D. V., Tolstikov A. S., Nauchniy vestnik NGTU, **2**, 39, 127–136.

Wübbena G., 1985: Software developments for geodetic positioning with GPS using TI 4100 code and carrier measurements. In: Proceedings of the 1st International Symposium on Precise Positioning with the Global Positioning System, Goad C. (Ed.), Rockville, MD, USA, April 15–19, 1985, 403–412.

Xu G., 2003: GPS Theory, algorithms and applications. Springer-Verlag Berlin Heidelberg New York, 315 p.

Zhalilo A. A., 2003: Carrier-Phase cycle – slip detection and repair of dual-frequency GPS data – new technique using correlation filtering principle. In: Proceedings of the 10th Saint Petersburg International Conference on Integrated Navigation System, St. Petersburg, Russia, May 26–28, 2003, 273–276.

Zhalilo A. A., Sadanova N. V., 2004: Carrier-phase cycle-slip detection, estimation and correction of dual-frequency GPS data – new efficient technique, algorithms and experimental results. Astronomy in Ukraine — Past, Present and Future: Abstract book, MAO-2004 Conference devoted to the 60th anniversary of the Main Astronomical Observatory of the National Academy of Sciences of Ukraine, July,15–17, Kiev, Ukraine, 154.

Zhalilo A. A., 2007: Carrier-phase cycle-slip detection and repair of single/dual-frequency GPS/GNSS observations – New universal technique and algorithms. In: Proceedings of 14th Saint Petersburg International Conference on Integrated Navigation Systems, St. Petersburg, Russia, 28–30 May, 2007, 293–302.